Astron. Astrophys. 309, 677–682 (1996)

ASTRONOMY AND ASTROPHYSICS

Atomic data from the IRON Project

XIV. Electron impact excitation of the Fe XIV fine-structure transition $^2P^o_{1/2}$–$^2P^o_{3/2}$

P.J. Storey[1], **H.E. Mason**[2], **and H.E. Saraph**[1]

[1] Department of Physics and Astronomy, Gower Street, London WC1E 6BT, England
[2] Department of Applied Mathematics and Theoretical Physics, Silver Street, Cambridge CB3 9EW, England

Received 31 July 1995 / Accepted 22 August 1995

Abstract. We calculate collision strengths and collision rates for electron excitation of the $^2P^o_{1/2}$–$^2P^o_{3/2}$ ground term fine-structure transition in Fe XIV, the coronal green line at 5303 Å. The collision strength for the green line is found to be strongly enhanced by resonances for the first 4 Rydberg above the excitation threshold, and as a result the collision rates are found to be significantly larger than other recently published results, even at coronal temperatures. The calculations are carried out using the R-matrix formulation of the close-coupling approximation.

Key words: atomic data – Sun: corona

1. Introduction

The Fe XIV green line (5303 Å) is the strongest forbidden line in the coronal visible spectrum. It has been observed extensively both during eclipses and with coronagraphs. Routine measurements of the green line have been made since the first coronagraph was constructed by B. Lyot in the 1930's. Synoptic observations are made at ground based observatories and several externally occulted coronagraphs have been flown on satellites (e.g. Skylab and the Solar Maximum Mission). The forthcoming Solar Heliospheric Observatory (SOHO) will carry a triple coronagraph (the Large Angle Spectroscopic Coronagraph - LASCO) to record White Light, Hα, Fe XIV, Fe X and Ca XV from 1.1R$_\odot$ to 30R$_\odot$. The importance of the Fe XIV ground term fine-structure transition extends far beyond the green coronal line. The population of the $3s^2$ $3p$ $^2P^o_{1/2}$ and $^2P^o_{3/2}$ levels also determines the electron density sensitivity of the Fe XIV UV lines. These have been studied from the solar atmosphere (e.g. OSO-7, Skylab, SERTS) and more recently from stellar atmospheres (EUVE). The SOHO will carry the Coronal Diagnostic Spectrometer (CDS), which covers the wavelength range 160–800 Å, and is designed to specifically study the coronal lines, including those from Fe XIV.

A review of the electron excitation data for Fe IX–Fe XIV was published by Mason (1994) as part of an atomic data assessment study for SOHO. Early work on Fe XIV was carried out using the Coulomb Born (CB) (Blaha 1971) and Distorted Wave (DW) approximation (Mason 1975). The latter calculation was limited in several ways. The collision strengths were only calculated at one energy value in the DW approximation with no account taken of the resonance structures. The target comprised only three configurations. Mason (1975) shows that the difference between the three configuration and nine configuration target gives rise to changes of 10%–50% in the oscillator strengths, which would be reflected in the collision strengths for dipole allowed transitions. Petrini (1969, 1970) carried out a detailed study of the electron excitation rate for the green coronal line. He calculated collision strengths using the close-coupling and the Coulomb Born I methods and used the quantum defect method to take account of the resonance structures.

Recent calculations for Fe XIV have been carried out by Dufton & Kingston (1991), using the R-matrix formulation of the close coupling (CC) approximation. These results are discussed in some detail by Mason (1994) and their main limitation was the restricted target (3 configurations) and omission of intermediate coupling below 10 Rydberg. Bhatia & Kastner (1993) published some DW collision strengths at 3 energy values, using a five configuration target. These represent a significant advance over Mason (1975), but do not contain any resonance contributions.

Recent work on other aluminium sequence ions (Saraph & Storey 1995) shows that the energy region between the first threshold and the $3s^2 3d$ ^2D term is dominated by series of resonances converging on terms of the target configurations $3s3p^2$, $3s^2 3d$ and $3s3p3d$. The need was perceived for a new calculation for Fe XIV in the CC approximation, with an accurate target

Send offprint requests to: P.J. Storey

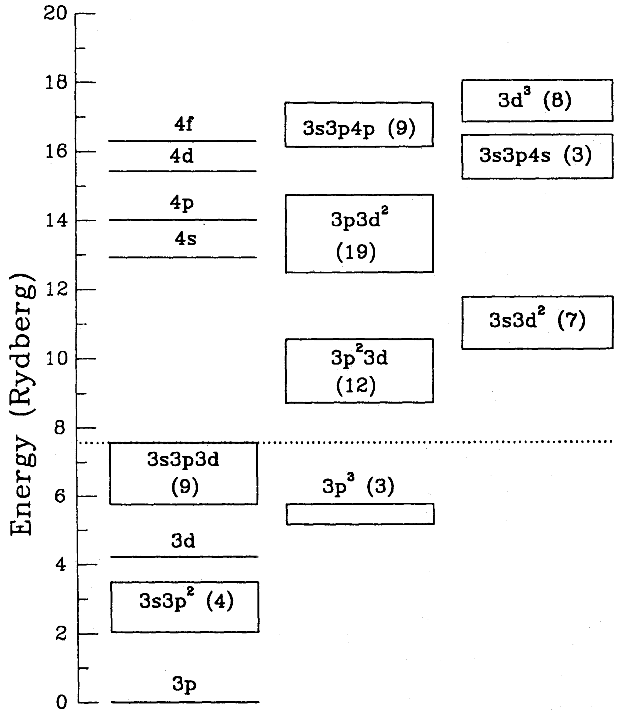

Fig. 1. Schematic energy diagram of Fe XIV. The numbers in brackets are the number of terms in each configuration. The dotted line shows the extent of the present target

which includes all these configurations. This work is part of the international collaboration known as the Iron Project (Hummer et al. 1993) whose aim is to make systematic calculations of electron-scattering cross-sections and rate coefficients for ions of astronomical interest, using the best available methods. The principal tool of the project is the atomic R-matrix computer code of Berrington et al. (1974, 1978) as optimised for use in the Opacity Project (Berrington et al. 1987). These codes have recently been extended (Hummer et al. 1993) so that collision strengths can be calculated at low energies, where some scattering channels are closed, including the effects of intermediate coupling in the target. Previous calculations have always neglected such effects. Results of calculations from the IRON Project will eventually be accessible from a public data base. At the moment, collision data can be obtained from the data bank maintained at Queen's University Belfast.

2. The target

For coronal ions, formed in conditions where collisional ionization by electrons determines the ionization balance, the mean thermal energy of the ambient electrons is several times greater than the ionization energy of the ion. The Fe^{13+} ion is abundant in the solar corona at temperatures of around 2×10^6 K and may be observed from plasmas with significantly higher temperatures (Arnaud & Raymond 1992). At 10^7 K, for example, free electrons with energies up to about 100 Rydberg are of importance in determining excitation rates. The ionization

Table 1. Configuration bases and potential scaling parameters used for the present Fe^{13+} target wave functions

The scattering target basis:

$3s^2\,3p$, $3s^2\,3d$, $3s\,3p^2$, $3s\,3p\,3d$, $3s\,3d^2$, $3p^3$, $3p^2\,3d$, $3p\,3d^2$, $3d^3$, $3s^2 4l$, $3s\,3p\,4l$, l=0,1,2,3

Potential scaling parameters:

1s	1.40465	2p	1.05182	3d	1.08479	4f	1.28406
2s	1.10939	3p	1.08085	4d	1.12220		
3s	1.11193	4p	1.09526				
4s	1.14882						

The expanded basis:

$3s^2\,3p$, $3s^2\,3d$, $3s\,3p^2$, $3s\,3p\,3d$, $3s\,3d^2$, $3p^3$, $3p^2\,3d$, $3p\,3d^2$, $3d^3$, $3s^2\,4l$, $3s\,3p\,4l$, $3p^2\,4l$, $3s\,3d\,4l$ l=0,1,2,3, $3p\,3d\,4s$, $3p\,3d\,4p$, $3s\,4s^2$, $3s\,4p^2$, $3s\,4s\,4p$

Potential scaling parameters:

1s	1.40444	2p	1.05178	3d	1.20079	4f	−0.88540
2s	1.11122	3p	1.24059	4d	−1.09886		
3s	1.33092	4p	−1.07273				
4s	−1.07273						

energy of Fe^{13+} is, by contrast, 28.8 Rydberg. No technique exists at present that permits a scattering calculation in which *all* states of the target can be incorporated, even approximately. A schematic diagram of the term structure of Fe XIV is shown in Fig. 1. The inclusion of all target states up to and including those of the form $3s^2 4l$, l=0,1,2,3, would generate a target of about 80 terms. Using existing codes, this would require an R-matrix scattering calculation which is beyond the limit of reasonable usage of current vector supercomputers, but is within the reach of parallel machines.

Work on other aluminium sequence ions (Saraph & Storey 1995) shows that the energy region between the first threshold and the $3s^2 3d\ ^2D$ term is dominated by series of resonances converging on terms of the target configurations $3s3p^2$, $3s^2 3d$ and 3s3p3d. We have therefore set out to construct target wave functions which describe these particular target states with reasonable accuracy, but which result in a computationally feasible scattering calculation. The target wavefunctions are expanded in a seventeen configuration basis, as listed in Table 1. Scattering channels are constructed from the five energetically lowest electron configurations giving rise to a scattering target of eighteen terms.

The target expansion includes all electron configurations of the $n = 3$ complex and those configurations including an $n = 4$ valence orbital which are energetically embedded within the $n = 3$ complex. We constructed the target wavefunctions using the program SUPERSTRUCTURE, (Eissner et al. 1974; Nussbaumer & Storey 1978), which uses radial wavefunctions calculated in a scaled Thomas-Fermi-Dirac statistical model potential. The scaling parameters were determined by the following

Table 2a. Energies of Fe^{13+} target terms in Rydberg. LS = pure LS-coupling, MD = with mass and Darwin terms, IC = intermediate coupling including one- and two-body relativistic interactions

Term		Exp.[a]	LS	MD	IC
$3s^23p$	$^2P^o$	0.	0.	0.	0.
$3s3p^2$	^4P	2.03897	1.875	2.024	2.015
	^2D	2.62460	2.477	2.625	2.630
	^2S	3.20884	3.127	3.282	3.250
	^2P	3.47459	3.342	3.502	3.520
$3s^23d$	^2D	4.20844	4.167	4.287	4.288
$3p^3$	$^2D^o$	5.15916	4.883	5.173	5.163
	$^4S^o$	5.25289	4.974	5.281	5.264
	$^2P^o$	5.75751	5.469	5.763	5.789
3s3p3d	$^4F^o$	—	5.604	5.860	5.856
	$^4P^o$	6.17603[b]	6.033	6.289	6.281
	$^4D^o$	6.26922	6.059	6.315	6.316
	$^2D^o$	6.42492	6.206	6.473	6.483
	$^2F^o$	6.75155	6.586	6.844	6.845
	$^2P^o$	7.24029[b]	7.127	7.391	7.382
	$^2F^o$	7.34772	7.209	7.469	7.472
	$^2P^o$	7.56099	7.428	7.696	7.704
	$^2D^o$	7.56759	7.434	7.697	7.706

[a] Redfors & Litzén (1989).
[b] Not all levels known experimentally.

Table 2b. Oscillator strengths for transitions in Fe^{13+}

Transition	Target basis		Extended basis	
	gf_L	gf_V	gf_L	gf_V
$3s^23p\ ^2P^o$–$3s3p^2\ ^2D$	0.381	0.390	0.375	0.385
–$3s3p^2\ ^2P$	0.325	0.299	0.319	0.324
–$3s3p^2\ ^2S$	2.477	2.438	2.457	2.522
–$3s^23d\ ^2D$	2.877	2.959	2.833	2.887

optimisation procedure, which was carried out in LS-coupling, i.e., neglecting all relativistic effects. First, the sum of the energies of all terms arising from the seventeen configurations was minimized, by varying the scaling parameters of the potentials of all ten orbitals. The scaling parameters for the $n = 4$ orbitals were then fixed and the energies of the eighteen lowest terms were minimized by varying the scaling parameters of the 1s, 2s, 2p, 3s, 3p and 3d orbitals. The resulting scaling parameters are also given in Table 1. This procedure was used to ensure that the wavefunctions of the $n = 4$ orbitals describe real physical states and are not optimised as correlation for the target states. Correlation orbitals give rise to resonances in the scattering cross-section at high energies which are of uncertain physical significance.

The energies of the eighteen target states are shown in Table 2a. The experimental values are taken from Redfors & Litzén (1989). We compare the experimental energies with three sets of calculated energies. The LS-coupled energies are calculated including only electrostatic interactions, while the intermediate coupling (IC) energies include one and two-body relativistic interactions as described in detail by Eissner et al. (1974). The third set of calculated energies, E_{MD}, includes only the one-body mass and Darwin relativistic energy shifts, no fine-structure terms. As discussed by Saraph & Storey (1996), this approximation results in term energies that are the same as those obtained in a full IC calculation provided that interactions between levels of different terms are negligible. Only for the terms $3s3p^2\ ^2S$, ^2P and 3s3p3d $^4P^o$, $^4D^o$ are such interactions important. Thus, for a highly charged ion where relativistic energy shifts are important, the energies E_{MD} provide a significantly better approximation than those obtained from pure LS-coupling. Using this approximation, however, the number of scattering channels is the same as it would be in LS-coupling, avoiding the large increase in computational cost incurred by doing the whole scattering calculation in intermediate coupling.

In Table 2b, we compare weighted electric dipole oscillator strengths for transitions from the ground term to the other target terms, calculated in both the length (gf_L) and velocity (gf_V) formulations. We give the results of two calculations. In addition to values obtained with the target configuration basis, we also give the results of a 30 configuration calculation, referred to as the extended basis, whose configurations are listed in Table 1. This basis includes more $n = 4$ correlation than the target basis, and was optimised on the energies of the six lowest states of Fe^{13+}. The $n = 4$ orbitals serve as correlation for these states and their radial functions were calculated in the scaled hydrogenic potentials described by Nussbaumer & Storey (1978). The potential scaling parameters derived from the optimisation are also given in Table 1. The aim of this extended calculation was to test the accuracy of the length oscillator strengths calculated with the target basis. The length results from the two bases agree within 2% for all four transitions.

3. The scattering calculation

The R-matrix method used in this calculation is described fully elsewhere (Hummer et al. 1993 and references therein). For this calculation, we use the version of the R-matrix code that incorporates those Breit-Pauli operators which lead to shifts of the term energies, but not those that lead to fine-structure (the MD approximation referred to above in the discussion of the target). The R-matrix boundary radius is chosen to be 4.66 au, at which point the most extended target orbital (4d) has declined to 0.13% of its maximum value. The expansion of each scattered electron partial wave is over a basis of 22 functions within the R-matrix boundary. The outer region calculation is carried out using the program STGFJ (Hummer et al. 1993), which calculates reactance matrices in LS-coupling and then transforms them into the Jk-coupling scheme (Saraph 1972, 1978), including the effects of intermediate coupling between the target terms, using the so-called term-coupling coefficients (TCCs). The scattering calculation includes all those partial waves that are necessary to ensure that this transformation is complete up to $J = 10$, for both even and odd parity.

The collision strength in the energy region between the $3s^23p\ ^2P^o$ and $3s3p^2\ ^4P$ thresholds was calculated at 10500 energy values, with an especially fine mesh at the lowest energies. Gailitis averaging was used when the energy was just below the ^4P threshold. In general, Gailitis averaging was used when the effective quantum number relative to the next threshold exceeded $\nu = 25$. For energies up to about 4 Rydberg, the collision strength is densely packed with resonances. It is not feasible to calculate the collision strength at a mesh sufficiently fine to delineate all such features. With a large number of resonances converging to many thresholds, it is reasonable to assume that the pattern of resonances with respect to positions and widths is essentially random so that the average collision strength can be obtained to reasonable accuracy with a mesh that does not delineate all features. We have therefore examined the convergence of the average collision strength as the number of mesh points is increased. For the energy region 0–2.039 Rydberg, the number of mesh points was progressively doubled until the average collision strength had converged to better than 1%. This was reached for 6400 points.

For the energy region 2.039–7.568 Rydberg, in which there are fifteen thresholds, a slightly different approach was used. The collision strength was calculated at 9000 equally spaced energy points covering this interval. The calculation was repeated for the same number of points with the starting position displaced by half the energy interval. Thus the second set of energies have no values in common with the first set. The average collision strengths obtained from these two calculations were 1.063 and 1.057 respectively. Finally the two sets of data were merged to give the collision strength in this energy region, with an average value of 1.060. From these tests we are confident that the purely statistical error on our results is of order 1% or less.

Finally, in the region of all channels open, the collision strength was calculated for energies up to 100 Rydberg at intervals of 1 Rydberg. The collision strength for higher energies is discussed below.

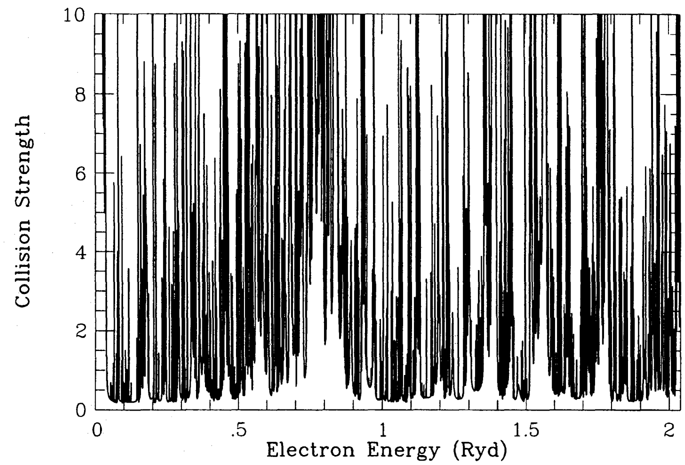

Fig. 2. The collision strength for the $^2P^o_{1/2}$–$^2P^o_{3/2}$ transition, between the $3s^23p\ ^2P^o$ and $3s3p^2\ ^4P$ thresholds

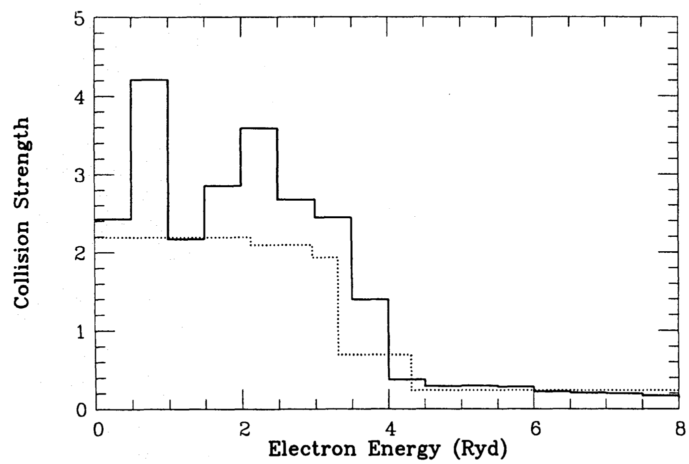

Fig. 3. The average collision strength for the $^2P^o_{1/2}$–$^2P^o_{3/2}$ ground-state fine-structure transition, in energy bins of 0.5 Rydberg. The dotted line shows the results of Petrini (1970)

3.1. The collision strength at high energies

As described above, the R-matrix scattering calculation included sufficient partial waves that the transformation to pair-coupling was complete up to $J = 10$. The contributions for higher J were then estimated assuming that the contributions from successive J decline in a geometric progression. For energies greater than 10 Rydberg it was found that the ratio of successive contributions Ω_J/Ω_{J-1} was not constant. The R-matrix calculation was therefore extended to $J = 12$ for energies greater than 10 Rydberg at which point a geometric decline is a reasonably good approximation. The correction to the total collision strength from this "top-up" procedure is 2% at 10 Rydberg and 17% at 100 Rydberg.

Including the top-up procedure, the total collision strength tends to a constant value of 0.165 above about 70 Rydberg. This can be compared with the limiting value of 0.186 calculated with a single configuration target, by Burgess et al. (1995, private communication) using the Born approximation. We note, however, that the quadrupole line strength for the $^2P^o_{1/2}$–$^2P^o_{3/2}$ transition in our 17 configuration target is a factor of 0.875 smaller than in a one configuration calculation. If we use the result of Burgess et al. (1995) and assume that the collision strength is proportional to the quadrupole line strength at high energy, we would expect a limiting value of 0.163, very close to our topped-up calculated result. In calculating collision rates for the $^2P^o_{1/2}$–$^2P^o_{3/2}$ transition, we have assumed that the collision strength has the constant value of 0.165 for all energies greater than 100 Rydberg.

4. Results and discussion

In Fig. 2, we show the collision strength between the $3s^23p\ ^2P^o$ and $3s3p^2\ ^4P$ thresholds. This energy region is dominated by resonances converging principally on the terms of the $3s3p^2$ and

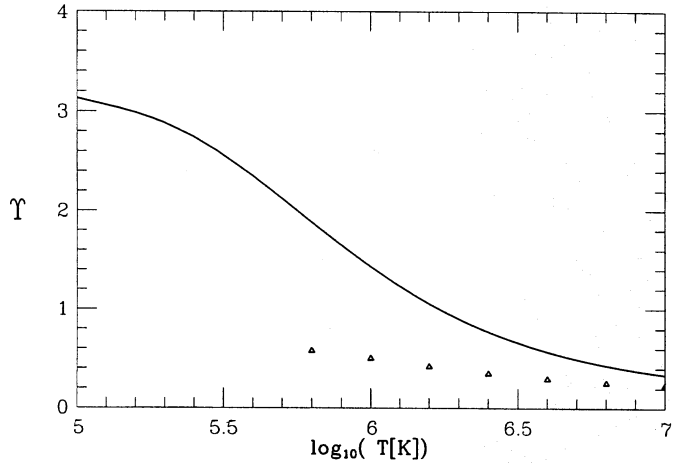

Fig. 4. The thermally averaged collision strength (Υ) for the $^2P^o_{1/2}$–$^2P^o_{3/2}$ ground-state fine-structure transition. Triangles are the results of Dufton & Kingston (1991)

$3s^23d$ configurations. In Fig. 3, we show the collision strength averaged over 0.5 Rydberg intervals up to 10 Rydberg. The average collision strength below 4 Rydberg is approximately 2.5, while above 4 Rydberg it is approximately 0.2.

Figure 4 shows the thermally averaged collision strengths from this work and from the work of Dufton & Kingston (1991). The effect of the large average collision strength in the first 4 Rydberg above threshold persists out to temperatures of at least 10^7 K. As a consequence the results in Fig. 4 are significantly larger than those obtained by any method that does not explicitly include resonance effects (Mason 1975; Bhatia & Kastner 1993).

The work of Dufton & Kingston (1991) however, does include resonances. Their thermally averaged collision strengths are rising toward lower temperatures, but are a factor 2–3× lower than ours (a factor of 2.86 at 10^6 K). They do not show their collision strength in the all-important region below 4 Rydberg, but we can infer from Fig. 4 that significant resonances were present. Their calculation included the target states, belonging to the electron configurations $3s3p^2$ and $3s^23d$, which give rise to the low energy resonances that dominate the collision rate. In order to understand the large discrepancy between their and our results we examined a number of possible error sources. One possible source of differences is in the representation of the target wave functions, but although they do not describe their target configuration basis in any detail, their calculated target term energies indicate that it was of reasonably high quality. Another possible explanation lies in the number of energies at which the collision strength was calculated. Dufton & Kingston (1991) used a mesh with 800 energy points in total, whereas we calculated collision strengths at 30 000 energy points in the resonance region. Our convergence tests, described in Sect. 4 above, indicated that too coarse a mesh does indeed underestimate the average collision strength in the resonance region, but a factor of 2–3 is still difficult to explain from these two differences. An examination of the collision data sent by Dufton & Kingston to the data bank at The Queen's University of Belfast revealed that there were no collision data stored at energies between the excitation threshold and that of target term $3s3p^2\ ^4P$. The omission of collision data from this important energy range would fully explain the shortfall of Dufton & Kingston's effective collision strength.

Table 3. Effective collision strengths

log (T[K])	Υ	log (T[K])	Υ
T = 0	10.410	4.8	3.326
1.0	10.550	5.0	3.128
1.2	10.639	5.2	2.984
1.4	10.791	5.4	2.741
1.6	11.063	5.6	2.351
1.8	11.595	5.7	2.120
2.0	12.619	5.8	1.882
2.2	14.377	5.9	1.648
2.4	16.937	6.0	1.429
2.6	19.796	6.1	1.229
2.8	21.948	6.2	1.052
3.0	22.746	6.3	0.899
3.2	21.994	6.4	0.768
3.4	19.663	6.5	0.657
3.6	16.190	6.6	0.565
3.7	14.286	6.7	0.489
3.8	12.414	6.8	0.427
3.9	10.656	6.9	0.376
4.0	9.066	7.0	0.335
4.1	7.674	7.5	0.221
4.2	6.493	8.0	0.183
4.3	5.524	9.0	0.167
4.4	4.762	10.0	0.165
4.6	3.784		

Of all the earlier calculations our results are in best agreement with the calculations of Petrini (1969, 1970). He used quantum defect methods to calculate the average collision strength below each threshold from CC or Coulomb-Born I reactance matrices above threshold. His results are shown as the dotted lines in Fig. 3.

In Table 3 we tabulate the thermally averaged collision strength for the $^2P^o_{1/2}$–$^2P^o_{3/2}$ ground state fine-structure transition in Fe XIV as a function of temperature, from 0–10^7 K. Note that the very low temperature results are much less reliable than those at coronal temperatures, since they depend critically on the positions of the near threshold resonances. In the collision strength for Fe XIV, there are very large resonance features within 0.05 Rydberg of the excitation threshold, whose positions are not known experimentally and whose calculated positions are sensitive to the details of the model, in particular to fine-structure effects that we have omitted. The uncertainties in the calculation of thermally averaged collision strengths at low temperatures have been explored in more detail elsewhere (Saraph & Storey 1996).

Acknowledgements. The IRON Project is grateful for support from PPARC through grant GR/H94979. P.J Storey is also in receipt of travel funds from NATO through grant CRG 941225.

References

Arnaud M., Raymond J.C., 1992, ApJ 398, 39

Berrington K.A., Burke P.G., Chang J.J., et al., 1974, Comput. Phys. Commun. 8, 149

Berrington K.A., Burke P.G., Le Dourneuf M., et al., 1978, Comput. Phys. Commun. 14, 367

Berrington K.A., Burke P.G., Butler K., et al., 1987, J. Phys. B: Atom. Mol. Phys. 20, 6379

Bhatia A.K., Kastner S.O., 1993, J. Quant. Spectrosc. Radiat. Transfer 49, 609

Blaha M., 1971, Sol. Phys. 17, 99

Dufton P.L., Kingston A.E., 1991, Physica Scripta 43, 386

Eissner W.E., Jones M., Nussbaumer H., 1974, Comput. Phys. Commun. 8, 270

Hummer D.G., Berrington K.A., Eissner W.E., et al., 1993, A&A 279, 298

Mason H.E., 1975, MNRAS 170, 651

Mason H.E., 1994, A.D.N.D.T., 57, 305

Nussbaumer H., Storey P.J., 1978, A&A 64, 139

Petrini D., 1969, A&A 1, 139

Petrini D., 1970, A&A 9, 392

Redfors A., Litzén U., 1989, J. Opt. Soc. Am. B. 6, 1447

Saraph H.E., 1972, Comput. Phys. Commun. 3, 256

Saraph H.E., 1978, Comput. Phys. Commun. 15, 247

Saraph H.E., Storey P.J., 1996, A&A 115, 151